24th COBEM - 2017

24th ABCM International Congress of Mechanical Engineering
December 3-8, 2017, Curitiba, PR, Brazil

COBEM-2017-1027
EFFECT OF WETTABILITY IN IMMISCIBLE DISPLACEMENT OF OIL ON MICROFLUIDIC POROUS MEDIA

Jorge Avendaño
Nicolle Lima
Antonio Quevedo
Marcio Carvalho
Pontifícia Universidade Católica do Rio de Janeiro, LMMP, Department of Mechanical Engineering, Rio de Janiero, Brazil
jorge@lmmp.mec.puc-rio.br, nicolle@lmmp.mec.puc-rio.br, toniokv2@gmail.com, msc@puc-rio.br

Abstract: *We present an original analysis on immiscible displacement of oil by water in microfluidic porous media of different wettability. Hydrophilic and hydrophobic identical micromodels saturated with a mineral oil were flooded with colored water at different flow rates until no more oil is produced. The complete extension of the micromodel after steady state was photographed for each experiment using an inverted microscope to precisely determinate residual oil saturation and ganglia size distribution. For the entire range of injection rates (Capillary number between $3.5x10^{-7}$ and $5x10^{-5}$) the hydrophobic porous medium exhibits a lower residual oil saturation, thus a better oil displacement, than its hydrophilic counterpart. We consider that the greater residual oil saturation in the hydrophilic porous media is a consequence of preferential patches of water (capillary fingering) that creates isolate islands of oil that cannot be reached. A higher quantity of very small oil ganglia is observed in the hydrophilic porous medium when compared to the hydrophobic but doesn't seem to positively affect the displacement because those very small ganglia will be trapped in the micromodel by capillary forces. On the other hand, a better displacement of oil in the hydrophobic porous media could be explained by the capillary driven snap-off that leads to poorly connected water paths that eventually modifies water relative permeability and improves the oil displacement efficiency.*

Keywords: *Wettability, Microfluidic, Residual oil saturation, Snap-Off, Capillary fingering*

1. INTRODUCTION

One of the most common methods on secondary oil recovery is waterflooding, which is usually performed before any other improved oil recovery method (Alvarado and Manrique, 2010). As water tends to displace oil trapped in the reservoir several variables and phenomena are involved (Abrams, 1975), depending on the reservoir affinity - oil-wet or water-wet - this immiscible displacement can be categorized as drainage or imbibition. Several studies on immiscible displacement in porous media (Bretherton, 1961; Saffman and Taylor, 1958; Lovoll et al., 2005; Wooding and Morel-Seytoux, 1976; Lenormand and Zarcone, 1984; Ramakrishnan and Wasan, 1984) have covered quite extensively the competition between viscous and capillary forces, commonly expressed in the effect of the Capillary number (*Ca*), but surrounded by the aforementioned variables that includes viscosity of the fluids, interfacial tension, flow rate, relative permeability, capillary pressure, porosity, porous media geometry and also wettability.

Regarding surface wettability, which is the main idea behind the present work, most experimental studies focuses on mixed or fractional wettability effect over residual oil saturation in core flooding experiences (McDougall and Sorbie, 1995; Shahidzadeh and Bonn, 2003; Dixit et al., 2000). In the other hand, simulation works tend to explore the trapping and displacing mechanisms that governs the flow in both drainage and imbibition in model porous media with fixed wettability (Blunt, 2001; Oren and Bakke, 2003; Zhao et al., 2010). A few experimental works explore the differences between hydrophilic and hydrophobic surfaces in well controlled surfaces. (Wu et al., 2012; Lee et al., 2015)

Studies - particularly in simulation of porous networks - have established two well-defined mechanisms of how displacement happens (Jamaloei et al., 2010; Lenormand and Zarcone, 1983; Dixit et al., 1996; Blunt, 1998). One is piston-lyke flow, where a high pressure drop moves "blocks of fluid" relatively evenly across the porous medium. The second is the snap-off mechanism (Olbricht, 1996), where an invasion of the wetting liquid in the vicinity of a throat eventually breaks the droplets of the displaced fluid that will be therefore easier to move. Theoretically, in situations where the surface is completely water or oil wettable (contact angles 0 and 180), the piston flow will be favored in

drainage experiments, while the snap-off will occur preferentially in imbibition experiments where the wetting fluid film theory (Bretherton, 1961; Pereira et al 1996) is also relevant as improves displacement.

Despite being a case study widely addressed, the results are still contradictory, therefore, in this work we focus on two well-controlled drainage and imbibition experiments (at various injection rates) on identical porous media completely water and oil wettable respectively, we will clearly show the influence of wettability on the entrapment of displaced fluid, which is evident in the ganglia morphology and differences in residual oil saturation. Later on, along with our results, we will discuss these mechanisms in more depth.

2. MATERIALS AND METHODS

The displacement experiments were performed on two "porous Media Chip", hereafter simply called hydrophilic and hydrophobic chip, produced by Dolomite Microfluidics. It models the structure of a porous rock with two different throat diameters (67 and 83 microns) and 110 micron straight channels that are randomly distributed throughout the device (Fig. 1). They have a nearly circular cross section (channel depth = 100 micrometers and channel width = 110 micrometers).

The pore volume and porosity of the microchip was obtained from image treatment, resulting 38 microliters and 68% respectively. The permeability was estimated in 86 D using Carman's relation (Carman, 1939).

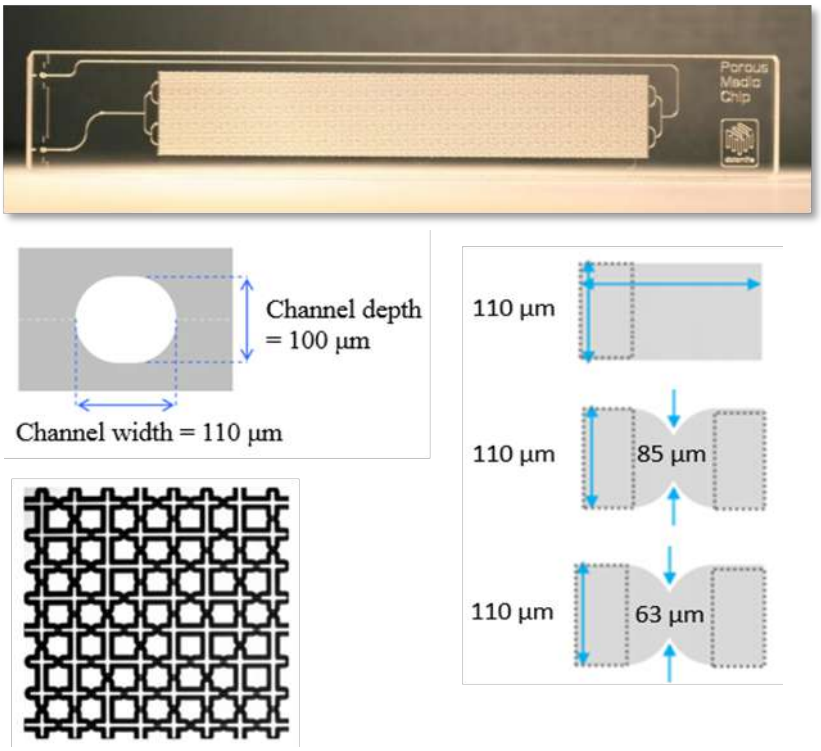

Figure 1: Porous Media Chip (2D): Configuration of the chip and the sizes of the constrictions

The fluid injection system consists of a syringe pump (Harvard Apparatus) used for injecting different fluids in the chip. All experiments were performed using glass syringes Hamilton Gastight, its termination in Teflon with Luer Lock coupling provided ease connection with the accessories used for the assembly of the injection setup. Three-way Solidor valves were used to establish the connection between the syringe and the microchip and also to control the flow, hoses with 1/32" internal diameter and special connectors for microfluidics complete the system.

The experimental setup also includes an inverted microscope (Axiovert 40Mat, Zeiss) for the visualization of the chip. The illumination was made using a light source from the top and the objective lens used has a magnification of 2,5X. A PixeLINK camera (PL-A662) was used to capture high-resolution videos and images (as shown on Fig. 2) of fluids within the network.

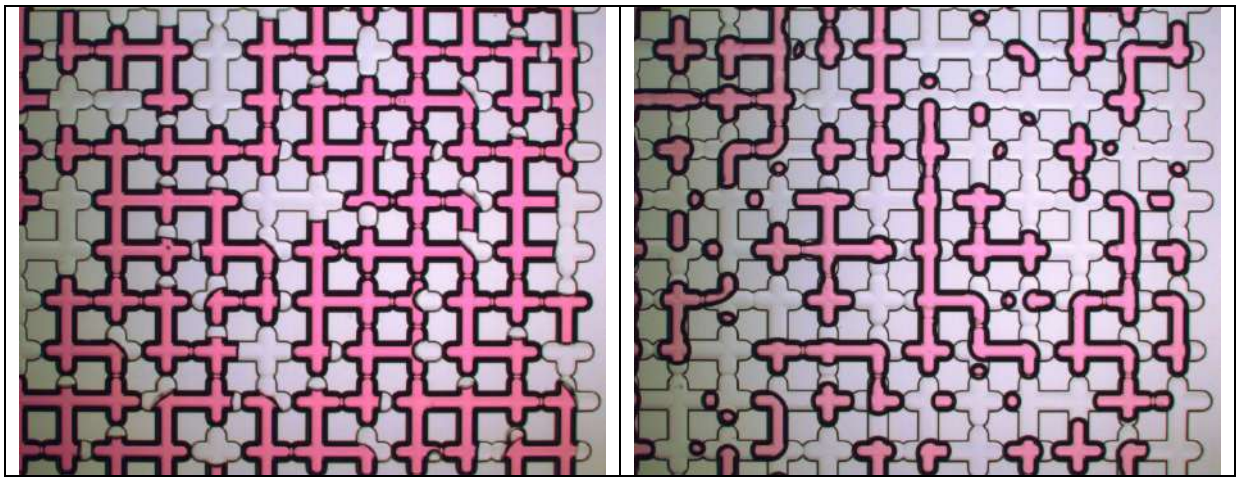

Figure 2: Comparison of oil and water ganglia in the same microchip zone after waterflooding in different treated surfaces (Left, hydrophilic. Right, hydrophobic) at the same flow rate of 4.16 ml/h after achieving steady state condition

The fluids used were: deionized colored water with red aqueous dye (μ=0.9 *cP* @ 25°C) and Drakeol 7 silicone oil (μ=17.8 *cP* @ 25°C) as displacing and displaced fluid respectively. The interfacial tension of colored water with Drakeol was measured (33.8 *mN/m*) finding a difference less than 2% compared to the interfacial tension using deionized water without colorant.

Using the syringe pumps, the chip is initially saturated with Drakeol 7. After that, the displacement experience begins setting a constant flow of colored deionized water. Different injection rates were performed in order to obtain a *Ca* sweep between $3.5x10^{-7}$ and $5x10^{-5}$ completing the injection of two porous volumes of water making sure that the residual oil saturation reaches a steady state. Once this condition is attained, we proceed to photograph the chip in sections using the inverted microscope (Fig. 3).

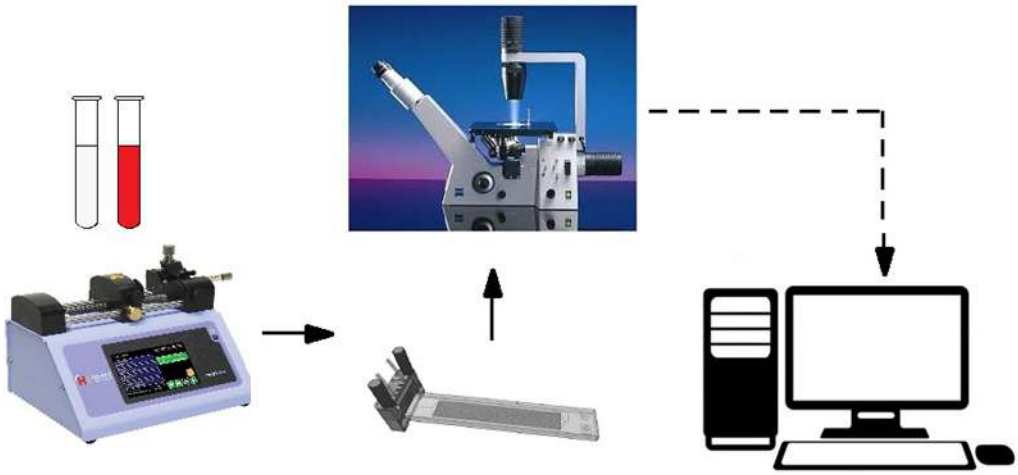

Figure 3: Experimental Setup

A critical part of our experiment is the image processing. The good contrast obtained between the fluids and the characteristics of the micromodel allowed us to develop a simple and effective procedure using ImageJ that not only allowed us to determine the residual oil saturation but also the morphology of the trapped oil ganglia.

3. RESULTS AND DISCUSSION

Tests were performed at different flow rates, to obtain $Ca_1 = 3.5x10^{-7}$, $Ca_2 = 7x10^{-7}$, $Ca_3 = 6x10^{-6}$ and $Ca_4 = 5x10^{-5}$. This work consists in a single experience of each chip at each flow rate, however, a duplicate test was performed using the hydrophilic chip obtaining a very good repeatability (similar residual oil saturation of 56% and 57% respectively). The summary of the experiences with the chips reconstructed from the photos is shown in Fig. 4.

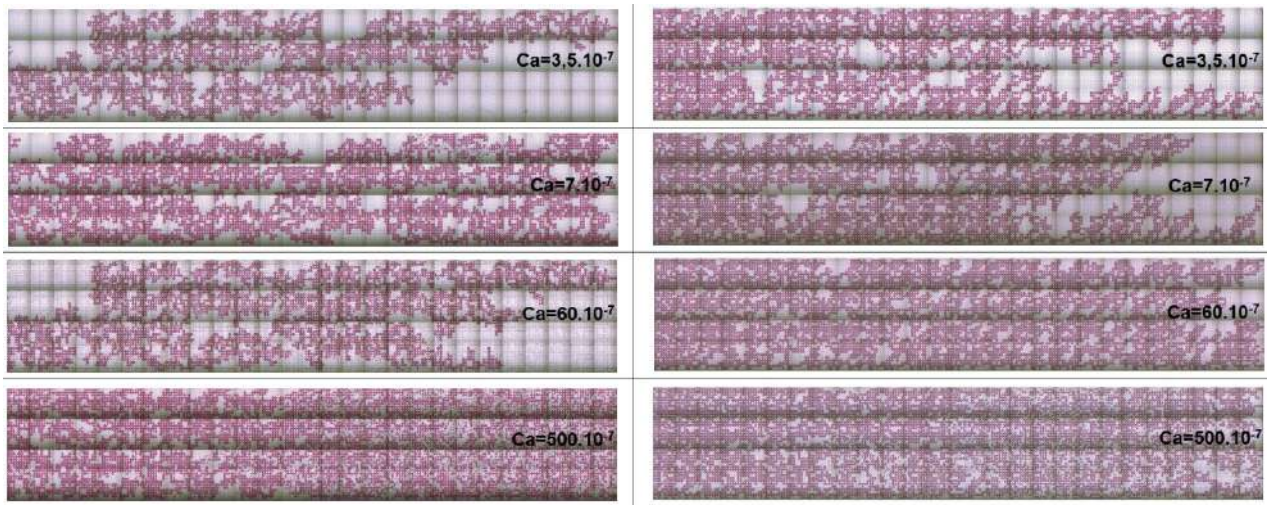

Figure 4: Macroscopic view of residual oil saturation after two porous volumes of water injected at different flow rates (Left: Hydrophilic Chip, Right: Hydrophobic Chip)

The first image treatment procedure developed consists in calculate the macroscopic residual oil saturation by simply adjusting the contrast to determinate the total water that invaded the chip (Fig. 5).

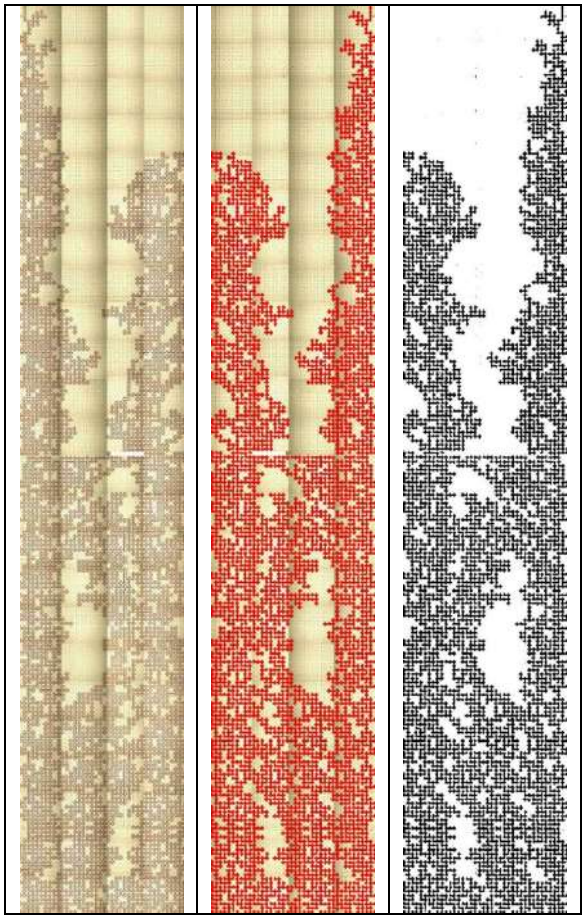

Figure 5: Example of image treatment for macroscopic residual oil calculations

At first sight, we verified differences in residual saturation when we compared the displacement of oil in porous media with different wettability. For the entire extension of capillary numbers studied, the oil recovery was better in drainage compared to imbibition, with marked differences at low Ca.

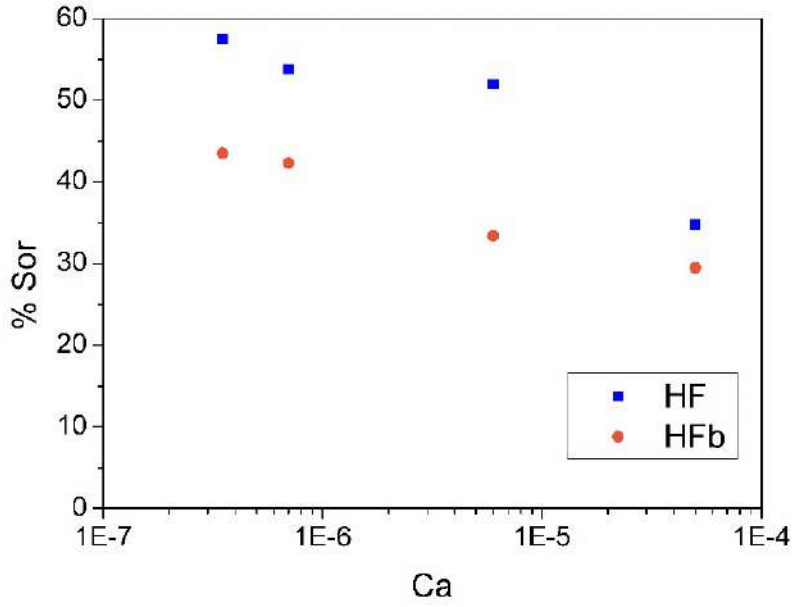

Figure 6: Residual oil saturation from displacement tests for hydrophilic (HF) and hydrophobic (HFb) tests

At low capillarity numbers, these results can be explained by the phenomenon of capillary fingering, clearly observed in Fig. 4, on the hydrophilic surface. It also surprises the low residual oil saturation in the hydrophobic medium at lower *Ca*, however, it seems to be explained by a capillary driven snap-off that favors a more uniform sweep along the chip.

Subsequently, we proceed to the microscopic analysis of the trapped ganglia. This is the most important contribution of our research, as in the past many assumptions (to feed simulations) and observations (usually in mixed wettability conditions) leaded to correlate microscopic entrapment with macroscopic residual saturation but in situations where wettability was difficult to control or no experimental data was available to support theories. For example, in Fig. 2, we can notice a very different oil entrapment pattern and consequently a very different water path when comparing drainage and imbibition experiences at the same flow rate and in the same region of both hydrophilic and hydrophobic chips.

A "unitary ganglia, UG" was defined (shown delimited b y a circle in Fig. 7) to generate a ganglia size distribution and thus enrich the discussion of the results. The second image treatment procedure then consists in generate the oil ganglia map (connected oil) all over the chip.

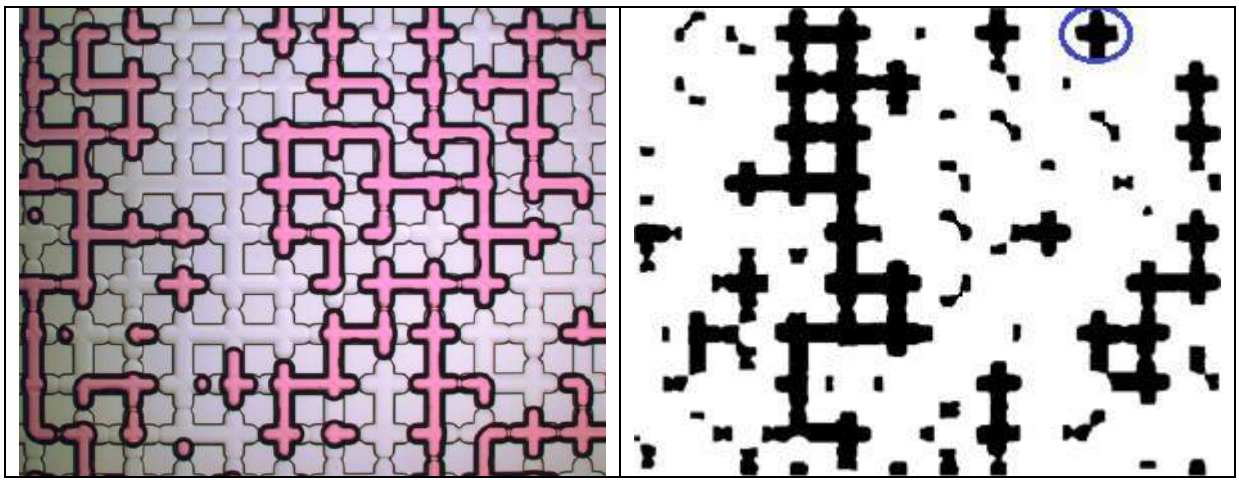

Figure 7: Left: Section of the porous media showing oil (transparent) trapped after water (red) flooding. Right: Oil ganglia (black) after image treatment. A “unitary ganglia” is shown delimited by a circle

The first result that drew a lot of attention in the microscopic analysis was the difference between the number of oil ganglia formed in each chips as a function of the capillary number. (Fig. 8)

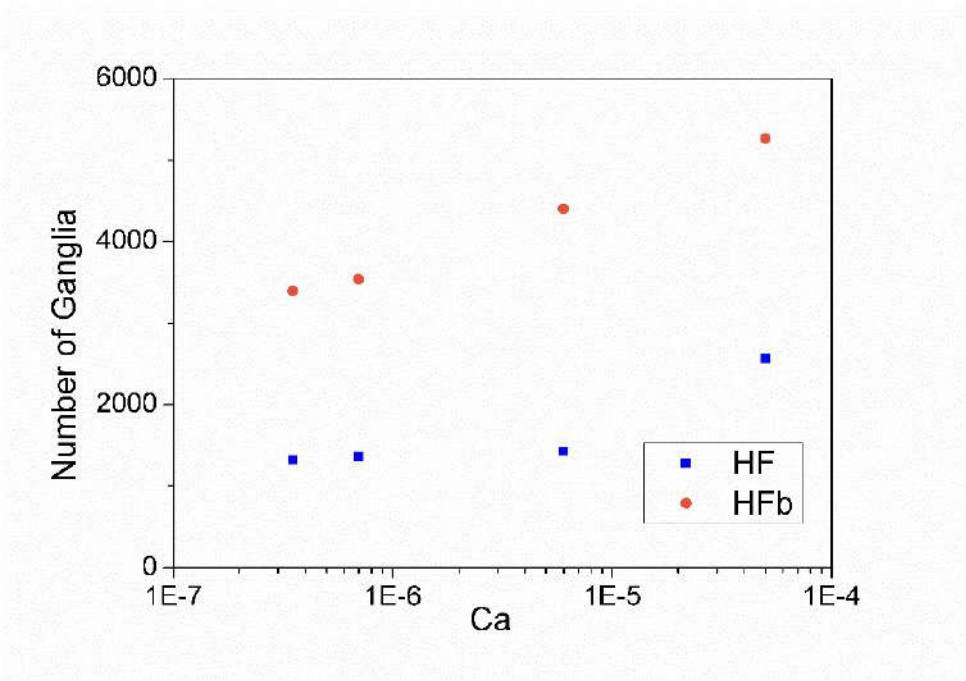

Figure 8: Number of oil ganglia after immiscible displacement in hydrophilic (HF) and hydrophobic (HFb) chips

This result is counterintuitive if we think of the potentially dominant mechanisms for the imbibition and drainage processes, since we would expect a greater number of ganglia in the imbibition process. However, we can attribute this effect to the snap-off in drainage, which initiate from the oil film attached to the channel walls, breaks the connection of the water paths and generate such a number of ganglia that lowers water relative permeability and finally improves the oil displacement efficiency.

In Figure 9 we show for each of the injection flows the size distribution of the trapped oil ganglia. There are considerable differences between both chips, which we can summarize as: 1) for the hydrophilic chip, there is a substantial number of very large ganglia (> 100UG), whereas for the hydrophobic surface these are almost non-existent, even from sizes equal to 31.6UG. 2) for the hydrophilic chip there is a vast number of very small ganglia (about 10% of the total ganglia in all cases), whereas on the hydrophobic surface this amount of very small ganglia barely reaches 1%.

These observations of microscopic analysis, reinforces the aforementioned theory of capillary driven snap-off, as in the hydrophobic surface, the large number of small ganglia are of ideal size to lower water relative permeability and consequently improve recovery, which is also favored by the absence of larger oil islands, which prevents to form because of the loss of hydraulic conductivity that prevails in the porous medium. In the hydrophilic case capillary fingering generates preferential paths implying a greater number of very large ganglia, these very large ganglia explain the high residual saturation, moreover, the size of the very small ganglia (which quantity is not negligible) is not enough to decrease water relative permeability along the chip, which could theoretically improve the recovery.

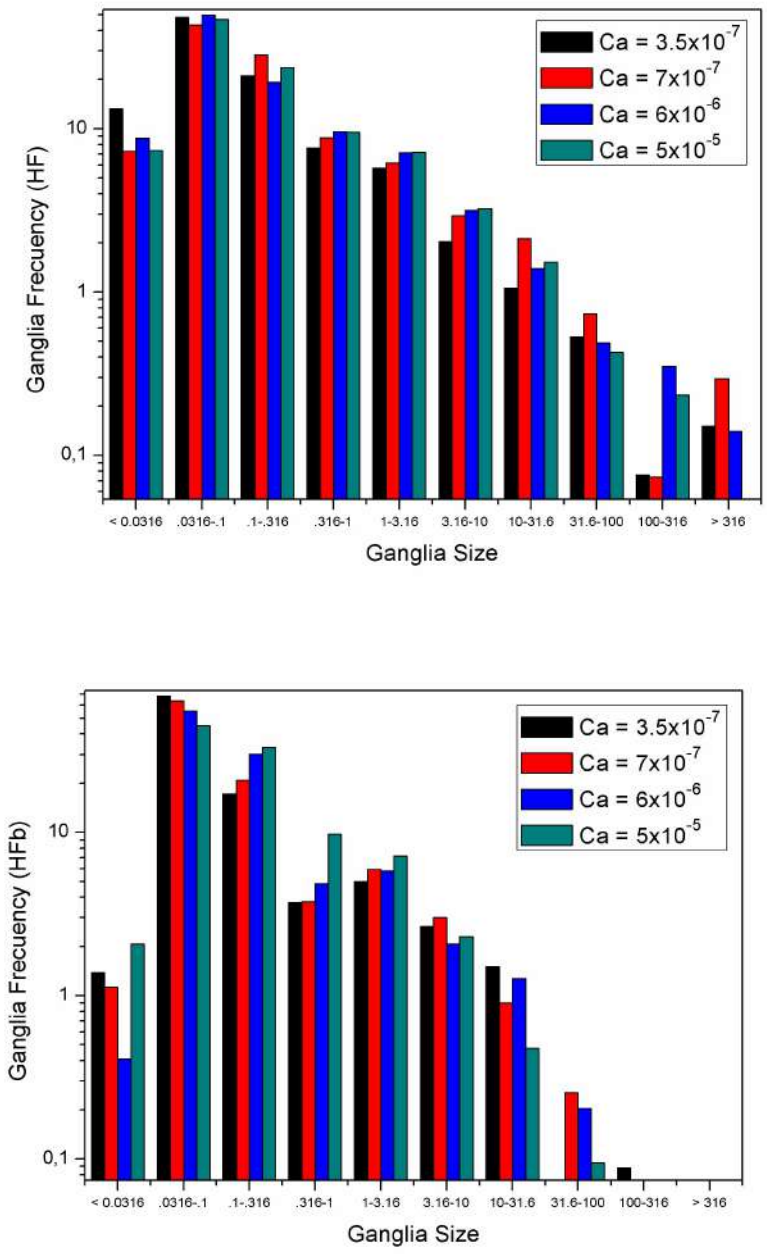

Figure 9: Ganglia size distribution of oil trapped in the hydrophobic (top) and hydrophilic (bottom) porous media chip

To complement the discussion, in Fig. 10 we analyze the amount of oil trapped as a function of the ganglia size for both chips, which only confirms our line of reasoning: almost all the oil trapped in the hydrophilic chip (about 80%, except the case of greater *Ca*) came from very large ganglia (> 100UG). In fact, only a significant decrease in residual oil saturation (Figure 6) happens when the flow is high enough to break the preferential patches (Figure 4, bottom left), which is comparable to the observation of Lovoll et al. (2005) where there is a transition between capillary and viscous fingering. In the case of the hydrophobic surface, less than 50% of the trapped oil comes from large ganglia (because there is just a few, and because they are not too large) which ultimately results in a minor overall residual saturation.

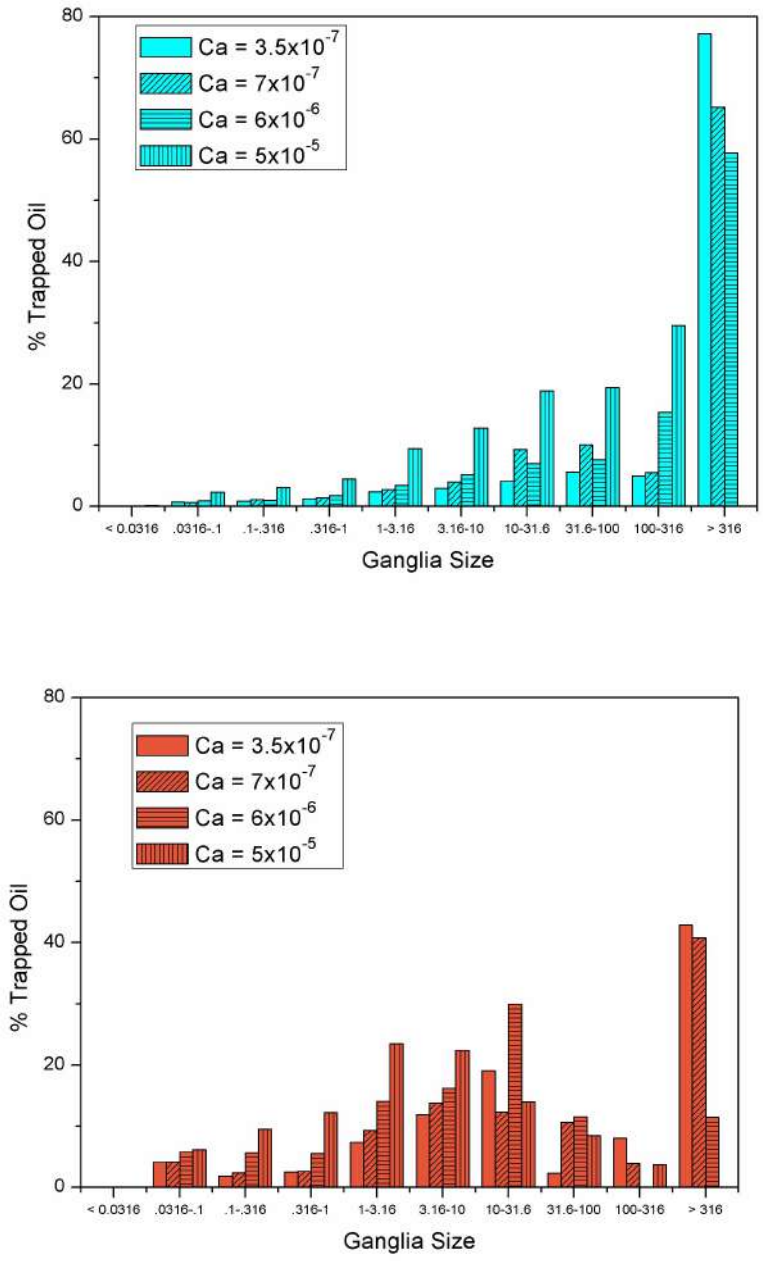

Figure 10: Trapped oil distribution along ganglia in the hydrophilic (top) and hydrophobic (bottom) porous media chip

4. CONCLUSIONS

With this work, where the conditions of wettability and multiphasic displacement were well controlled, we could verify that in the studied *Ca* range, oil recovery in a porous model is more efficient under drainage conditions (hydrophobic surface) than under imbibition conditions (hydrophilic surface). Analyzing the morphological distribution of the residual oil ganglia, we can conclude that capillary driven snap-off in the hydrophobic porous medium, even at very small *Ca* values influences the sweep positively. On the other hand, the recovery is very negatively influenced in the hydrophilic porous media by the formation of preferential paths of the displacing fluid.

5. ACKNOWLEDGEMENTS

This work was funded by Repsol-Sinopec Brasil.

6. REFERENCES

Abrams, 1975. "The Influence of Fluid Viscosity, Interfacial Tension, and Flow Velocity on Residual Oil Saturation Left by Waterflood," *Soc. Pet. Eng. J.*, vol. 15, no. 5, pp. 437-447.

Alvarado and Manrique, 2010. "Enhanced oil recovery: An update review," *Energies*, vol. 3, no. 9, pp. 1529-1575.

Blunt, 2001. "Flow in porous media - Pore-network models and multiphase flow," *Curr. Opin. Colloid Interface Sci.*, vol. 6, no. 3, pp. 197-207.

Blunt, 1998. "Physically-based network modeling of multiphase flow in intermediate-wet porous media," *J. Pet. Sci. Eng.*, vol. 20, no. 3-4, pp. 117-125.

Bretherton, 1961. "The motion of long bubbles in tubes," *J. Fluid Mech.*, vol. 10, no. 2, p. 166.

Carman, 1939. "Permeability of saturated sands, soils and clays," *J. Agric. Sci.*, vol. 29, no. 2, p. 262.

Dixit et al., 2000. "Empirical measures of wettability in porous media and the relationship between them derived from pore-scale modelling," *Transp. Porous Media*, vol. 40, no. 1, pp. 27-54.

Dixit et al., 1996. "Pore Scale Modelling of Nettability Effects and Their Influence on Oil Recovery," *SPE.* February, pp. 501-515.

Lee et al., 2015. “Photopatterned oil-reservoir micromodels with tailored wetting properties”. *Lab Chip*. pp. 3047-55.

Lenormand and Zarcone, 1984. "Role of Roughness and Edges During Imbibition in Square Capillaries," *Proc. SPE Annu. Tech. Conf. Exhib.*, p. 17.

Lenormand et al., 1983. "Mechanisms of the displacement of one fluid by another in a network of capillary ducts," *J. Fluid Mech.*, vol. 135, October, p. 337.

Løvoll et al., 2005. "Competition of gravity, capillary and viscous forces during drainage in a two-dimensional porous medium, a pore scale study," *Energy*, vol. 30, no. 6, pp. 861-872.

McDougall and Sorbie, 1995. "The Impact of Wettability on Waterflooding: Pore-Scale Simulation," *SPE Reserv. Eng.*, vol. 10, no. 3, pp. 208-213.

Olbricht, 1996. “Pore-scale prototypes of multiphase flow in porous media”. *Ann. Rev. Fluid Mech*. vol. 28, pp. 187-213.

Oren and Bakke, 2003. "Reconstruction of Berea sandstone and pore-scale modelling of wettability effects," *J. Pet. Sci. Eng.*, vol. 39, no. 3-4, pp. 177-199.

Pereira et al., 1996. "Pore-scale network model for drainage-dominated three-phase flow in porous media," *Transp. Porous Media*, vol. 24, no. 2, pp. 167-201.

Ramakrishnan and Wasan, 1984. "The Relative Permeability Function for Two-Phase Flow in Porous Media: Effect of Capillary Number," *SPE*. Oil Recovery Symposium, 15-18 April, Tulsa.

Saffman and Taylor, 1958. "The Penetration of a Fluid into a Porous Medium or Hele-Shaw Cell Containing a More Viscous Liquid," *Proc. R. Soc. A Math. Phys. Eng. Sci.*, vol. 245, no. 1242, pp. 312-329.

Shahidzadeh and Bonn, 2003. "Gravity drainage in porous media: the effect of wetting," *J. Pet. Sci. Eng.*, vol. 39, no. 3-4, pp. 409-416.

Wooding and Morel-Seytoux, 1976 "Multiphase fluid flow through porous media," *Annu. Rev. Fluid Mech.*, vol. 8, no. 1, pp. 233-274.

Wu et al., 2012. "Single- and two-phase flow in microfluidic porous media analogs based on Voronoi tessellation," *Lab Chip*, vol. 12, no. 2, pp. 253-261.

Jamaloei et al., 2010. "Pore-scale events in drainage process through porous media under high- and low-interfacial tension flow conditions," *J. Pet. Sci. Eng.*, vol. 75, no. 1-2, pp. 223-233.

Zhao et al., 2010. "Pore-scale modeling: Effects of wettability on waterflood oil recovery," *J. Pet. Sci. Eng.*, vol. 71, no. 3-4, pp. 169-178, 2010

7. RESPONSIBILITY NOTICE

The authors, J. Avendaño, N. Lima, A. Quevedo and M. Carvalho, are the only responsible for the printed material included in this paper.